Solid-supported membrane technology for the investigation of the influenza A virus M2 channel activity

ARTICLE *in* PFLÜGERS ARCHIV - EUROPEAN JOURNAL OF PHYSIOLOGY · NOVEMBER 2009

Impact Factor: 4.1 · DOI: 10.1007/s00424-009-0760-1 · Source: PubMed

Pflugers Arch - Eur J Physiol (2010) 459:593–605
DOI 10.1007/s00424-009-0760-1

Solid-supported membrane technology for the investigation of the influenza A virus M2 channel activity

Victoria Balannik · Petr Obrdlik · Samsoon Inayat · Catrin Steensen · Jun Wang · Joshua M. Rausch · William F. DeGrado · Bela Kelety · Lawrence H. Pinto

Received: 18 August 2009 / Revised: 29 September 2009 / Accepted: 29 October 2009 / Published online: 28 November 2009

Abstract Influenza A virus encodes an integral membrane protein, A/M2, that forms a pH-gated proton channel that is essential for viral replication. The A/M2 channel is a target for the anti-influenza drug amantadine, although the effectiveness of this drug has been diminished by the appearance of naturally occurring point mutations in the channel pore. Thus, there is a great need to discover novel anti-influenza therapeutics, and, since the A/M2 channel is a proven target, approaches are needed to screen for new classes of inhibitors for the A/M2 channel. Prior in-depth studies of the activity and drug sensitivity of A/M2 channels have employed labor-intensive electrophysiology techniques. In this study, we tested the validity of electrophysiological measurements with solid-supported membranes (SSM) as a less labor-intensive alternative technique for the investigation of A/M2 ion channel properties and for drug screening. By comparing the SSM-based measurements of the activity and drug sensitivity of A/M2 wild-type and mutant channels with measurements made with conventional electrophysiology methods, we show that SSM-based electrophysiology is an efficient and reliable tool for functional studies of the A/M2 channel protein and for screening compounds for inhibitory activity against the channel.

Keywords Influenza A virus · A/M2 channel · Proton channel · SSM-based electrophysiology · Technology · SURFE^{2}R

Introduction

Influenza A has one of the highest infection rates among human viruses, and during unpredictable pandemics, is

Victoria Balannik and Petr Obrdlik contributed equally to this work.

Electronic supplementary material The online version of this article (doi:10.1007/s00424-009-0760-1) contains supplementary material, which is available to authorized users.

V. Balannik · J. M. Rausch · L. H. Pinto (✉)
Department of Neurobiology and Physiology,
Northwestern University,
Hogan Hall, 2205 Tech Drive,
Evanston, IL 60208-3500, USA
e-mail: larry-pinto@northwestern.edu

P. Obrdlik · C. Steensen · B. Kelety
IonGate Biosciences,
65926 Frankfurt/Main, Germany

S. Inayat
Department of Biomedical Engineering McCormick School of Engineering, Northwestern University,
Evanston, IL 60208-3500, USA

J. Wang · W. F. DeGrado
Department of Chemistry, University of Pennsylvania,
Philadelphia, PA 19104-6059, USA

W. F. DeGrado
Department of Biochemistry and Biophysics, School of Medicine,
University of Pennsylvania,
Philadelphia, PA 19104-6059, USA

Present Address:
J. M. Rausch
Department of Chemistry, Elmhurst College,
Elmhurst, IL 60126-3296, USA

likely to kill millions [1]. Influenza A virus encodes an integral membrane protein A/M2 that forms a proton channel that is essential for virus replication [2, 3]. The channel is gated by decreased pH of the extracellular medium bathing the N-terminal of this type III integral membrane protein [4]. The channel serves to acidify the virion prior to uncoating and in some cases shunts the acidification of the acidic Golgi apparatus to prevent premature conformational change of hemagglutinin [5]. The channel is capable of acidifying mammalian cells and oocytes in which it is expressed and passes steady proton currents; it is not inactivated for as long as 30 min [4]. The A/M2 protein is considered to be one of the smallest bona fide ion channels. The channel consists of four identical subunits of 97 amino acids [6]. Each subunit consists of a short periplasmic ectodomain (23 residues), a single membrane spanning region (20 residues) and a cytoplasmic endodomain (53 residues). The highly conserved HxxxW motif located in the transmembrane region of the protein is responsible for the channel activity and proton selectivity [6, 7]. The A/M2 ion channel is the target of the anti-influenza drug amantadine, although resistance to this drug dramatically increased over the past years as a result of the formation of amantadine-insensitive A/M2 phenotypes [8–10]. All the amantadine-resistant mutants carry naturally arising point mutations of the pore-lining residues of the outer transmembrane domain of the A/M2 protein [10], and solid-state nuclear magnetic resonance (NMR) spectroscopy has shown that resonances of the outer pore-lining residues are modified by amantadine binding [11]. A/M2-S31N and A/M2-V27A are the most widespread amantadine-insensitive mutants of the influenza A virus [8, 12, 13]. Unfortunately, until now there are no potent inhibitors of the amantadine-insensitive A/M2 mutant channels. Thus, there is a great need to discover novel anti-influenza therapeutics and the A/M2 channel protein is a proven target.

The activity and the drug sensitivity of A/M2 channels have been widely studied using conventional electrophysiology techniques [14–16]; however, these measurements are technically challenging and time consuming. In this study, we tested the validity of electrophysiological measurements with solid supported membranes (SSM) as an alternative technique for the investigation of A/M2 ion channel properties.

For the SSM-based measurements, the SSM consists of a di-phytanoyl-phosphatidyl-choline deposited on an alkane-thiol monolayer which in turn rests on a thin layer gold electrode as previously described [17, 18]. Membrane fragments or vesicles containing the protein of interest are then adsorbed onto the SSM, thereby forming a fluid compartment between the membrane fragments and the SSM that is separated from the bulk solution [18]. The protein-specific charge movements into or out of this compartment are evoked by substrate, or ligand concentration jumps, as appropriate. The resulting protein-dependent charge translocation is measured as a transient electrical current. The transient properties of the current are based on the arrangement of the protein-containing membranes, the fluid compartment, and the SSM on the sensor [18]. In this arrangement, the SSM behaves like a capacitor with the lipid and the alkane-thiol layers being the dielectric, whereas the solution in the fluid compartment and the gold electrode are the capacitor plates. Accordingly, the charging of the SSM capacitor depends on the transport activity of the assayed protein. So far, SSM-based electrophysiology has been successfully used for the functional characterization of several membrane transporter proteins [19–23]. Here, we show that SSM-based electrophysiology is an efficient and reliable tool for functional studies of the A/M2 channel protein.

Results

For the SSM-based electrophysiological assay, A/M2 channels were transiently expressed in CHO-K1 cells. A/M2 protein-containing CHO-K1 membranes were prepared by sucrose gradient centrifugation and adsorbed on the SSM-coated sensor as discussed in "Materials and methods". A/M2 channel activity was evoked by rapid exchange of the non-activating solution (pH 7.0) with the activating solution (pH 6.0), and the response was detected as a transient positive electrical current (Fig. 1a, upper black trace). It is presumed that the CHO cell membranes expressing the M2 protein were adsorbed in random orientation, and thus, that only those presenting the extracellular, N-terminal region of the M2 protein to the bathing solution were activated. The transient nature of the proton-induced currents was in agreement with the principles of the SSM-based electrophysiology, in which the protein-specific currents correspond to the charging of the SSM capacitor [18]. The positive sign of the current was consistent with the movement of positive charge towards the sensor electrode. A ring of four histidine residues at position 37 in the TM domain has been shown to be a site of proton storage for the M2 protein [7]. The currents decayed in the range of several hundred milliseconds after the application of the activating solutions. The rate of decay of these transients was slower than for SSM measurements of channels with higher single channel conductance [24]. After the current decayed, the system was set back by rinsing the sensor in the non-activating solution. The application of the non-activating solution induced a negative transient current corresponding to the proton back flow/discharging of the sensor. Following this solution exchange protocol, stable A/M2 protein signals

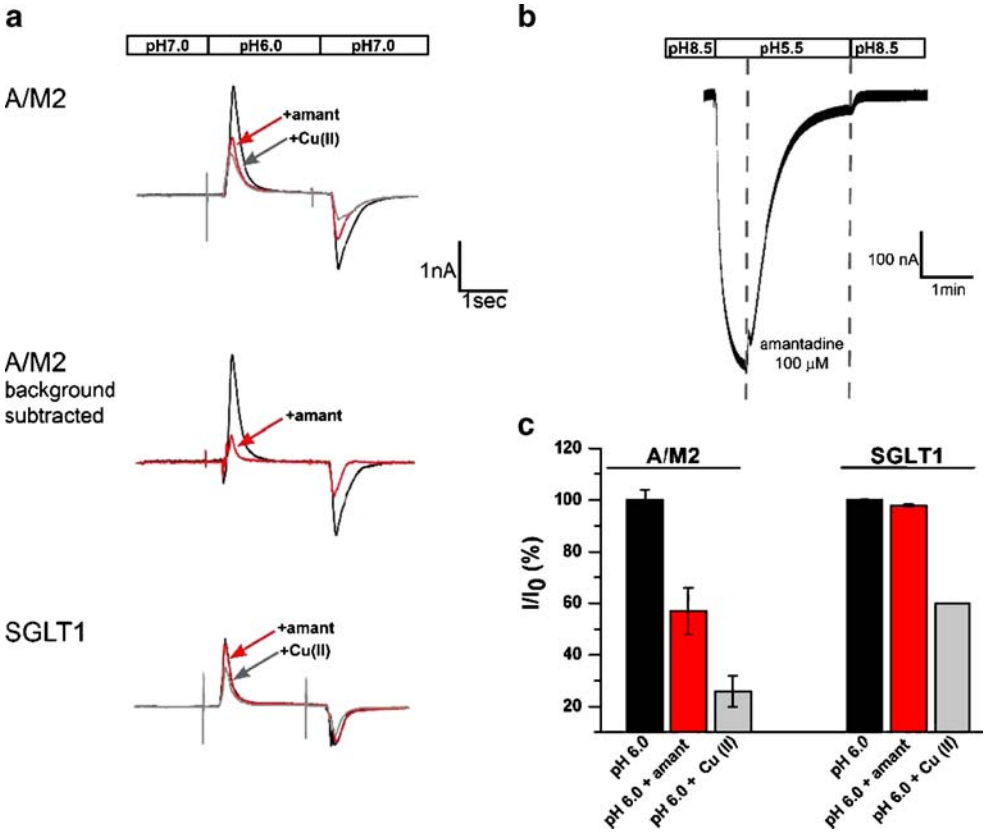

Fig. 1 A/M2 channel protein-specific activity and inhibition measured using SSM-based technology and TEVC. **a** Representative traces of the electrical activity measured on sensors covered with either CHO-K1 cell membranes expressing A/M2 protein, or CHO-K1 membranes expressing the rabbit glucose transporter rbSGLT1 as a control. The activity was measured in a response to a rapid exchange of the non-activating solution (pH 7.0) for the activating solution (pH 6.0; *black traces*). These transient, capacitive currents decayed within several hundred milliseconds after the application of the activating solutions. After the current decayed, the system was returned to its original condition by rinsing the sensor in the non-activation solution. The application of the non-activation solution induced a negative transient current corresponding to the proton back flow/discharging of the sensor. The A/M2 channel activity was selectively inhibited by amantadine (100 μM) and by $CuSO_4$ (Cu(II), 25 μM; *red and gray traces*, respectively). The *middle trace represents* the levels of A/M2 channel activity and amantadine inhibition after Cu(II)-insensitive background current was subtracted. **b** Representative trace of the A/M2 channel activity measured from A/M2 expressing *Xenopus* oocytes using TEVC. A/M2 inward H^+ current was induced by application of the activating solution (pH 5.5). After the maximal channel activity was achieved, currents were inhibited by the application of amantadine (100 μM; *first vertical interrupted line*) in the activating solution for 2 min. The channel activation was resumed by switching back to the non-activating solution (pH 8.5; *second vertical interrupted line*). Note that in contrast to the SSM recordings, the oocyte recordings give a steady inward current that can be sustained indefinitely (note the longer time scale in **b** than in **a**) as long as the pH gradient across the oocyte membrane is maintained because the TEVC apparatus provides for a closed circuit for current to flow, whereas the SSM membrane is able to be charged but charge flow through the channel does not lead to a sustained current since the underlying SSM does not allow a current flow between gold electrode and reference electrode. **c** Summary of the results shown in **a**. The channel activity corresponds to the peak current amplitudes measured upon application of the activation solution (pH 6.0; see **a**). Responses in the presence of the inhibitor (*I*) were normalized to the current evoked by the application of the activating (pH 6.0) solution without inhibitor (I_0). Each *bar* is a mean (±SD) of three to five independent experiments

could be repeatedly detected over an extended time period (4–6 h). Since the assay conditions of the forward reaction are much better defined than the conditions of the reverse reaction, only the activating solution-induced peak current amplitudes were used to analyze the protein's ion channel activity. A/M2 channel activity was inhibited by the application of the A/M2-specific inhibitor amantadine (100 μM) in the non-activating (pH 7.0) and the activating (pH 6.0) solutions (Fig. 1a, upper red trace); however, the inhibition level was significantly lower both from that measured in A/M2 expressing CHO-K1 cells using the whole-cell configuration of the patch-clamp technique [25] and from that measured in A/M2 expressing oocytes using TEVC (Fig. 1b). In order to address the difference in the amantadine inhibition levels between the two assays, SSM-adsorbed A/M2 channels were exposed to $CuSO_4$ (25 μM) in the activating solution. It has been previously shown that Cu(II) is capable of inhibition of A/M2 channel activity by interacting with the His37 residue of the HxxxW gating motif in the channel pore [26]. Cu(II) was shown to inhibit

both wild-type A/M2 channels and amantadine-insensitive point mutant channels (that occur distal to the HxxxW motif) [26]. SSM-based A/M2 activity was efficiently inhibited by the application of $CuSO_4$ (25 μM) in the activating solution (Fig. 1a upper gray trace). As a control experiment, SSM-coated electrodes adsorbed with CHO-K1 cell membranes expressing the rabbit glucose transporter rbSGLT1 were exposed to the same solution exchange protocol, to which electrodes adsorbed with the A/M2 expressing membranes were exposed (Fig. 1a, bottom traces). When charge translocation was measured for the control membranes, the response to pH jumps was much smaller than for the A/M2 expressing membranes. Moreover, the response of the control membranes to acidification was amantadine insensitive (Fig. 1a, bottom black and red traces). However, control currents were partially inhibited by $CuSO_4$ (25 μM) indicating that copper at this concentration is capable of partially inhibiting the endogenous electrical activity of the CHO-K1 cell membranes (Fig. 1a bottom gray trace). For comparison, a current recording from an oocyte expressing the A/M2 ion channel protein is shown in Fig. 1b. In contrast to the SSM recording, the oocyte recording shows a sustained current because the TEVC apparatus provides a return pathway for current flow.

In order to get a better understanding of the amantadine and copper sensitivities of the currents, we performed a quantitative analysis of the pH-evoked current amplitudes. In general, the total current amplitudes were stable on individual sensors but could vary between different A/M2 or control sensors. Therefore, for the quantitative analysis, the currents in the presence of an inhibitor were normalized to the currents before the inhibitor application on each individual sensor. The quantitative analysis of the amantadine and copper-sensitive currents (Fig. 1c) demonstrated that the pH-induced activity on the SGLT1 control sensors were significantly less sensitive to copper than the corresponding currents on the A/M2 sensors.

Based on the above findings, we concluded that the copper-insensitive component may be considered to be a background electrical activity, unrelated to the A/M2 channel activity, and thus may be subtracted from the total current measured for the electrodes adsorbed with membranes expressing A/M2 protein. After the subtraction of the copper-insensitive background currents, the fraction of A/M2 channel activity inhibited by amantadine became comparable to reported values (Fig. 1a, middle traces). Using the SSM-based assay, we also tested the pH-induced activity of A/M2 channel proteins reconstituted in liposomes. Empty control liposomes did not show any detectable currents upon acidification (Electronic supplementary material).

The A/M2 channel conducts protons with high selectivity [15, 27]. Figure 2a shows that for the A/M2 channels expressed in *Xenopus* oocytes, the reversal potentials (Vrev) determined from the I–V relation in Na^+-, or K^+-based

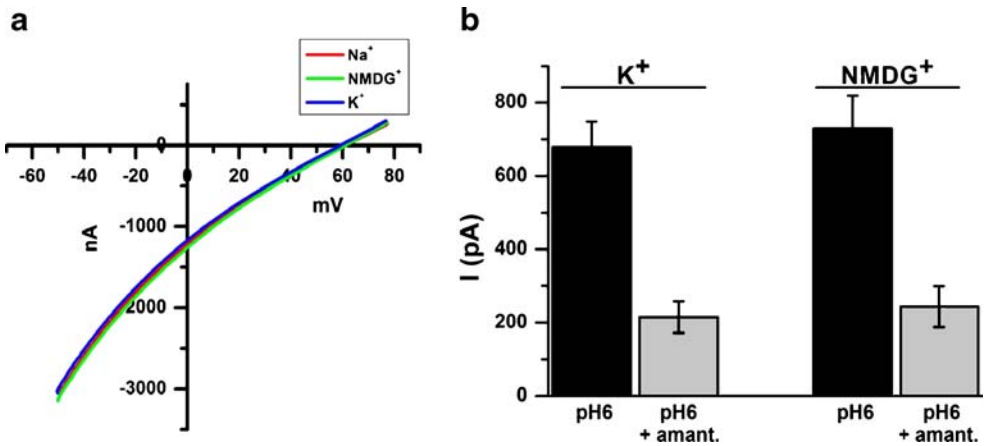

Fig. 2 SSM-based technology is capable of measuring the proton flow through the A/M2 channel protein. **a** Representative trace of the current-voltage relationship (*I/V*) of A/M2 channel activity measured in *Xenopus* oocytes. A/M2 channels were activated by the application of the acidic bathing medium (pH 5.5) for 10 s, and the channel activity was assayed applying the voltage ramp from −60 to +80 mV to obtain an I/V curve (see "Materials and methods" for details). The channel activity was assayed first in the Na^+-based medium (*red trace*). After 3 min recovery at pH 8.5, the channel activity was assayed again in the $NMDG^+$-based medium (*green trace*), and finally after 3 min recovery at pH 8.5, an additional trace of activity was measured in the K^+-based medium (*blue trace*). The Vrev of the A/M2 channels measured in Na^+, in $NMDG^+$, or in K^+-based medium were found to be comparable, indicating high proton selectivity of the channel. **b** A/M2 channel activity and amantadine (100 μM) sensitivity measured with SSM-based technology. Either using the standard solutions with K^+ (140 mM, see "Materials and methods") or solutions in which $NMDG^+$ was substituted for K^+. To allow the comparison of the channel activity in the two bathing solution A/M2 channels coming from the same SSM-adsorbed sensor were first activated by the K^+-based solution and then by the $NMDG^+$-based solution. The currents are shown after the subtraction of the Cu(II)-insensitive background component. Each *bar* is the mean (±SD) of four activations on two independent experiments. Note, that the amount of channel activity measured in $NMDG^+$-based solutions is indistinguishable from the amount of channel activity in K^+-based solutions

activating (pH 5.5) and non-activating solutions (pH 8.5) are similar to the Vrev measured in the solutions based on presumably impermeable cation N-methyl-D-glucamine$^+$ ($NMDG^+$). Thus, assuming that the electrical activity detected in the SSM-based assay for A/M2 channels corresponds to the movement of protons only, substitution of $NMDG^+$ for K^+ in the activating and the non-activating solutions should have no significant effect on the measured channel activity, when applied on A/M2 channels adsorbed on the same sensor. Figure 2b shows that with the SSM-based assay, A/M2 channels were activated to the same extent by activating solution containing K^+ as they were by the solution in which monovalent cations were replaced with $NMDG^+$, which is consistent with the electrophysiological measurements. Amantadine sensitivity of the A/M2 currents in the presence of $NMDG^+$ did not differ significantly from that measured in K^+-containing solution (Fig. 2b). The above result demonstrates that SSM-based assay reflects A/M2 proton channel activity found with conventional electrophysiology.

Amantadine-inhibition potency (measured as IC_{50}) for wild-type A/M2 channels was also tested using SSM-based technology. Figure 3a shows the dose-inhibition curve for amantadine measured with SSM-adsorbed A/M2 expressing membranes (solid squares, IC_{50}=0.3 μM and with A/M2 protein expressed in *Xenopus* oocytes (open squares, IC_{50}=16.3 μM). The isochronic amantadine-inhibition curve for A/M2 ion channels expressed in oocytes shows lower sensitivity of the channel to the drug than the curve obtained for the SSM-based assay. The higher IC_{50} value observed in oocytes reflects the fact that the rate of amantadine binding is very slow when A/M2 is expressed in this cell type [28]. It is not experimentally easy to measure the binding at equilibrium, so the degree of inhibition is conventionally measured after a constant incubation time of 2 min. When the concentration of drug is in the low micromolar range, binding is not complete on this time frame, leading to artificially high IC_{50} value. Indeed, if the degree of inhibition is measured after 1 h, then 0.4 μM amantadine is sufficient to cause 50% inhibition of the A/M2 protein from the A/Udorn/72 strain of influenza A virus [28],very close to the IC_{50} value of 0.3 μM measured for isolated membranes using the SSM-based technology. Thus, we hypothesize that the difference in the IC_{50} values between the two experimental systems probably resulted from the differences in the equilibration rates for A/M2 expressing isolated CHO-K1 cell membranes versus A/M2 channels expressed in oocytes. To test this idea further, we first used the whole-cell configuration of the patch-clamp technique to examine the relative amantadine inhibition in A/M2 expressing CHO-K1 cells, as this would be more directly comparable to the measurements done in oocytes.

When measured by the patch-clamp technique, the A/M2 channel sensitivity to amantadine after 2-min incubation was somewhat higher in the cultured CHO-K1 cells than in oocytes, showing approximately 50% inhibition at 5 μM drug concentration (Fig. 3b). Moreover, amantadine concentrations of 1–5 μM are consistently effective for the inhibition of viral replication in influenza A-infected cultured cells [10] and for the inhibition A/M2 proteins reconstituted in liposomes [29, 30]. These finding indicate that the precise value of the IC_{50} for amantadine depends on the experimental system and the degree to which

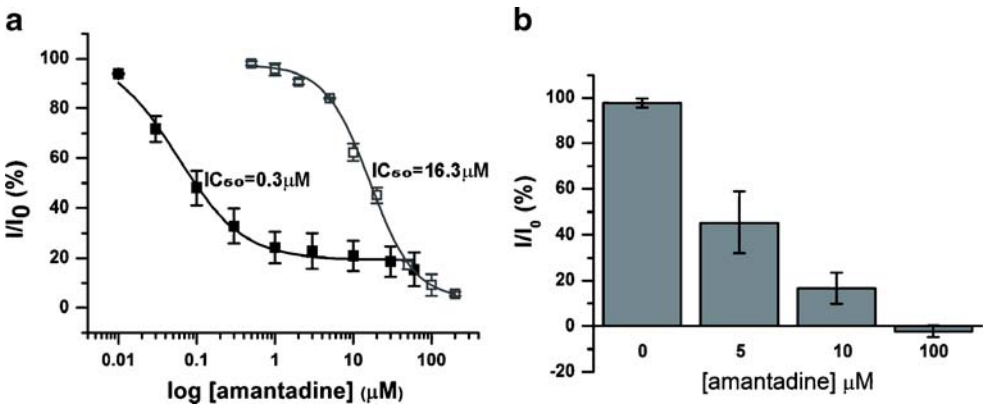

Fig. 3 Concentration-dependent inhibition of A/M2 channel activity by amantadine measured by SSM-based and conventional electrophysiology. **a** Dependence of the channel activity on the concentration of amantadine. *Solid squares* represent measurements from sensors covered with A/M2-containing CHO-K1 cell membranes (IC_{50}= 0.3 μM). *Open squares* represent TEVC measurements from *Xenopus* oocytes expressing the A/M2 protein. The isochronic dose-response curve for A/M2 expressing oocytes was determined for 2-min long amantadine incubations (IC_{50}=16.3 μM). Each point is a mean (±SD) of three to five independent experiments. **b** Inhibitory effect of different amantadine concentrations (5, 10, and 100 μM) on A/M2 channels expressed in CHO-K1 cells and measured with the whole-cell configuration of the patch-clamp technique. The channel activity after preincubations with amantadine (5 min, 5, 10, and 100 μM) (*I*) was normalized to the current evoked by application of the activating (pH 6.0) solution without inhibitor (I_0). Each *bar* is a mean (±SD) of three to five independent experiments

equilibration is reached on the timescale of the measurement. We therefore examined further the reversibility and kinetics of equilibration.

In 1978, Skehel et al. showed that amantadine inhibition of influenza A virus replication is reversible in no longer than 1 h [31]. However, the rate of reversibility of amantadine inhibition of A/M2 channels expressed in heterologous systems has never been directly addressed. When tested in the SSM-based assay, A/M2 inhibition by amantadine rapidly reversed on a scale of 15–20 min (Fig. 4a), while the reversibility rate strongly depends on the internal parameters of the solution exchange of the SSM experimental setup and may be much faster in the systems with the continuous solution flow. The rate of amantadine inhibition reversibility measured in the SSM-based assay is faster than that previously observed in A/M2 expressing

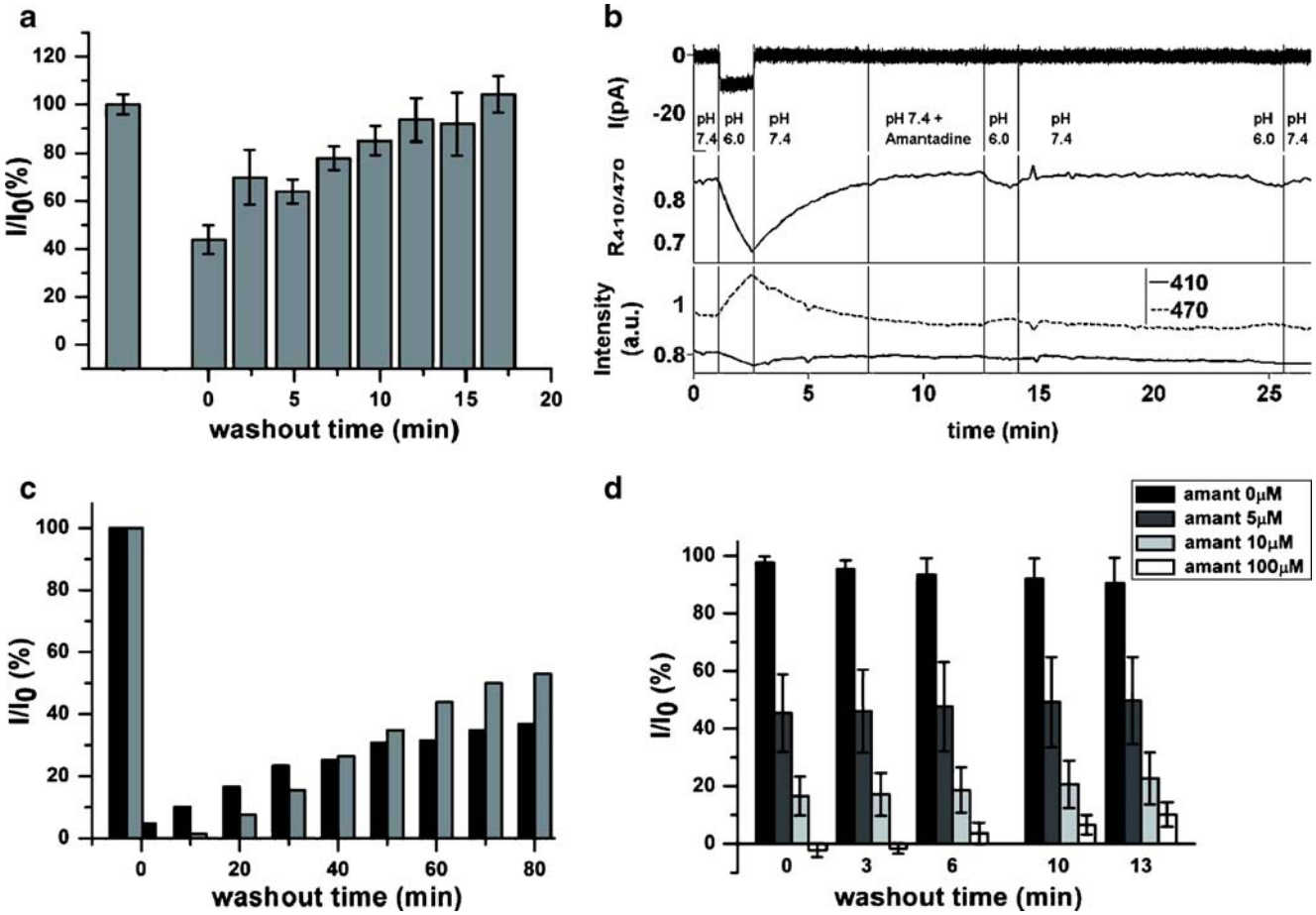

Fig. 4 Comparison between the amantadine reversibility rates measured in SSM-based and conventional electrophysiological assays. **a** Time course of the recovery of A/M2 channel activity from amantadine (100 μM) inhibition measured in the SSM-based assay. First, the A/M2 channels were activated in absence of the inhibitor and then in presence of amantadine (100 μM, t=0). Afterwards, the sensor was washed with the non-activating solution (pH 7.0) and the channel activity was then sampled again in the absence of amantadine. Responses after the inhibitor removal (I) were normalized to the initial currents evoked by the application of the activating (pH 6.0) solution without inhibitor (I_0). The channel activity corresponds to peak currents. Each *bar* is a mean (±SD) of six independent experiments. **b** Representative trace of A/M2-pHluorin channel activity and the resulting cellular acidification in CHO-K1 cells. Amantadine inhibition and amantadine washout were measured by the patch-clamp technique in the whole-cell configuration—*upper panel*, current recording. *Middle panel*—the 410/470 nm excitation ratio ($R_{410/470}$) calculated for the patched cell upon A/M2-pHluorin channel activation, amantadine inhibition and washout. *Bottom panel*—representative traces of the pHluorin emission at 410 and 470 nm excitation wavelengths for the patched cell. **c** Time course of the recovery of A/M2 channel activity after amantadine removal (100 μM). *Black bars* correspond to the TEVC measurements from A/M2 expressing *Xenopus* oocytes. *Gray bars* correspond to the whole-cell patch-clamp measurements from A/M2 expressing CHO-K1 cells. Responses after the inhibitor removal (I) were normalized to the initial currents evoked by the application of the activating (pH 5.5 for oocytes and pH 6.0 for CHO-K1 cells) solution without inhibitor (I_0). **d** Time course of the recovery of A/M2 channel activity after the removal of amantadine of various concentrations (5, 10, and 100 μM, respectively). The measurements were done on A/M2 expressing CHO-K1 cells using the whole-cell configuration of the patch-clamp technique. Responses after the inhibitor removal (I) were normalized to the initial current evoked by the application of the activating (pH 6.0) solution without inhibitor (I_0). Each *bar* is a mean (±SD) of three to five independent experiments

oocytes, which shows very little reversal during the first 5 min after drug removal [25, 32]. However, no data were available for longer amantadine washout times for recombinant A/M2 channels. In order to address the differences between the rates of amantadine reversibility in SSM-based assay results and previous studies, we performed simultaneous measurements of the electrical activity and the cell acidification rates for A/M2 expressing CHO-K1 cells. For this set of experiments, the pH-sensitive mutant of green fluorescent protein (pHluorin, [33]) was fused to the C-terminus of A/M2 subunits through a 15 amino acid helical linker to produce a chimeric A/M2-pHluorin protein. The A/M2-pHluorin construct was transiently expressed in CHO-K1 cells and the A/M2 channel activity was assayed using the patch-clamp technique in the whole-cell configuration. The electrical activity of the fused protein was not significantly different from that of the wild-type A/M2 channel. Simultaneously with electrophysiological measurements of A/M2 activity, the change in the cytopasmic pH of the recorded cell was detected. For those measurements, we employed the dependence of pHluorin excitation ratio at 410/470 nm ($R_{410/470}$) upon pH (pH range, 5.5–7.5). Figure 4b shows that neither A/M2 current recovery, nor cytoplasmic acidification occurs for the first 13 min after channel inhibition by 100 μM amantadine.

To test further the rate of amantadine reversibility on recombinant A/M2 channels, we performed prolonged electrophysiological measurements during amantadine washout. For this experiment, A/M2 channels expressed either in *Xenopus* oocytes or in CHO-K1 cells were first activated by application of a low pH-activating solution (pH 5.5 for oocytes and pH 6.0 for CHO-K1 cells). Then, low pH-evoked currents were inhibited by amantadine (100 μM). After the maximal inhibition was achieved (2 min for oocytes and 5 min for CHO-K1 cells), the cells were superfused with the non-activating solution (pH 8.5 for oocytes and pH 7.4 for CHO-K1 cells) and the recovery of A/M2 activity was monitored by repeated brief activations for another 80 min. As shown in Fig. 4c, after washout of the drug, A/M2 channel activity was slowly reversible in both *Xenopus* oocytes (black bars), or for CHO-K1 cells (gray bars). The time-dependent increase in activity of the channel is well described by a rising exponential, consistent with a pseudo-first-order process. The half-time observed in CHO-K1 cells was 70±10 min, which is significantly slower than for isolated membranes from the same cell type. The corresponding value for A/M2 expressed in oocytes was approximately 100 to 150 min, confirming previous findings of very slow reversal in this cell type [28].

The dissociation of the drug from the A/M2 protein is expected to be a first-order process, which indicates that the same slow rate of reversal should occur over a wide range of initial degrees of inhibition, elicited by differing initial concentrations of the inhibitor. Thus, we tested the effect of amantadine concentration on the recovery from inhibition of A/M2 channel activity in A/M2 expressing CHO-K1 cells. A/M2 channel activity was evoked by application of activating solution (pH 6.0); then, the channel activity was inhibited by amantadine at 5, 10, or 100 μM. The recovery of A/M2 current from the inhibition was assayed for 13 min after the removal of amantadine. Full recovery was not achieved for any amantadine concentration tested (Fig. 4d), indicating that even at lower amantadine concentrations the inhibitor washout rates measured in the electrophysiological assays were slower than the amantadine washout rates with the SSM-based assay.

A/M2-S31N and A/M2-V27A are among the most widespread amantadine-resistant mutants of the influenza A virus [8, 12, 13]. Until recently, there were no anti-viral drugs that could inhibit the amantadine-resistant mutants. Recently, we have investigated a new anti-viral compound spiro[5.5]undecan-3-amine (spiran amine), which was shown to inhibit A/M2 wild-type and A/M2-V27A amantadine-resistant mutant channels, but not the A/M2-S31N mutant [34]. In order to test whether the SSM-based assay can be applied for anti-viral drug screening, we tested the inhibition potency of amantadine and of spiran amine on SSM-adsorbed CHO-K1 cell membranes expressing either A/M2-S31N, or A/M2-V27A mutant channels (Fig. 5a). The inhibition measured using the SSM-based assay was similar to that measured in *Xenopus* oocytes using TEVC (Fig. 5b). As shown in Fig. 5, there was no significant difference between the inhibition potencies of amantadine and spiran amine on wild-type and mutant A/M2 channels measured in the two assays.

We have widened the screening experiments to nine additional compounds for which inhibition potency on A/M2 channel activity was previously tested using conventional electrophysiology. Among them there were the well-known A/M2 channel inhibitors like BL-1743 [35] and adamentol [36], as well as some recently synthesized drugs [16, 34]. The inhibition patterns for those compounds measured using the SSM-based assay were comparable to those measured using TEVC on A/M2 expressing *Xenopus* oocytes (Table 1).

Discussion

In the current study, we validated the use of SSM-based electrophysiology for the investigation of A/M2 channel activity and the potential of this approach for screening for channel activity modulators. In order to validate the SSM-based electrophysiology, we first tested the channel-specific features of the A/M2 protein with the SSM-based

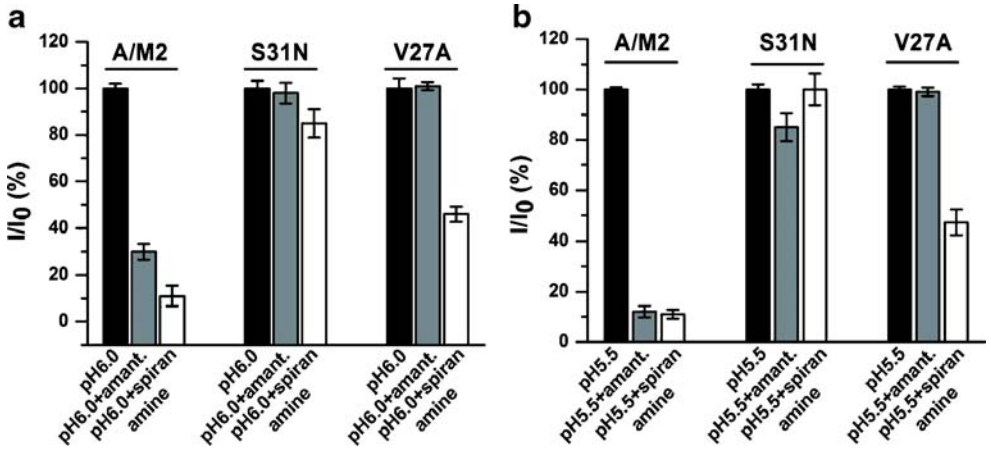

Fig. 5 The effect of spiran amine on the activity of A/M2 wild-type and amantadine-insensitive mutants. **a** and **b** Inhibition of A/M2, A/M2-S31N, and A/M2-V27A channel activity with amantadine (100 μM, *gray bars*) and spiran amine (spiro[5.5]undecan-3-amine, 100 μM, *white bars*). **a** Measurements performed on SSM electrodes covered with the CHO-K1 cell membranes expressing the appropriate A/M2 protein. The currents are shown after the subtraction of the Cu (II)-insensitive background component. Responses in the presence of the inhibitor (*I*) were normalized to the currents evoked by the application of the activating (pH 6.0) solution without inhibitor (I_0). (See "Materials and methods" for the descriptions of drugs applications). Each *bar* is a mean (±SD) of four measurements performed in two independent experiments. **b** Measurements performed on *Xenopus* oocytes expressing the appropriate A/M2 protein using TEVC (see also Fig. 3a). Responses in the presence of the inhibitor (*I*) were normalized to the currents evoked by the application of the activating (pH 5.5) solution without inhibitor (I_0). Each *bar* is a mean (±SD) of seven to ten independent experiments

technique and compared them to the results obtained with conventional electrophysiology. Then we compared the inhibition potencies of various chemical compounds on A/M2 when measured using SSM-based and conventional electrophysiology. The following A/M2 channel-specific features were addressed: (1) activation of the channel by extracellular acidification; (2) inhibition of the channel activity by A/M2 specific inhibitors; (3) ion selectivity of the channel; (4) inhibition patterns of amantadine-sensitive and amantadine-insensitive mutants; (5) inhibition potencies of various anti-viral compounds on wild-type A/M2 channels.

A/M2 channel-specific activation and inhibition A/M2 channel activity measured with the SSM-technology in the response to pH jumps was inhibited by A/M2 channel-specific inhibitors amantadine and $CuSO_4$ at saturating concentrations (100 μM and 25 μM correspondingly; Fig. 1). The endogenous pH-induced activity of CHO-K1 control cell membranes was found to be significantly lower than the activity of A/M2 expressing membranes and was completely amantadine insensitive as expected. CHO-K1 cell endogenous currents were partially inhibited by $CuSO_4$ (25 μM; Fig. 1). This partial inhibition of the endogenous CHO-K1 cell activity by Cu(II) may be explained by

Table 1 Inhibitory potency of various compounds on A/M2 as measured with SSM-based assay and with TEVC

Compound	A/M2 activity (%) after inhibition with 100 μM of each compound	
	SSM-based assay	TEVC
2-[3-azaspiro [5, 5] undecanol]-2-imidazoline (BL 1743)	36.1±2.4	25.5±3.8
3-azaspiro [5, 5] undecane	22.4±4.2	5.0±1.3
1,5-deoxa-9-azaspiro [5, 5] undecane	88.3±7.6	97.1±4.2
N-methylspiro [5, 5] undecan-3-aminium chloride	5.6±1.2	8.8±1.9
N-(spiro [5, 5] undecan-3-yl) propane-1,3-diamine	85.2±4.8	95.1±2.1
1-(spiro [5, 5] undecan-3-yl) guanidine	36.7±6.7	8.4±3.7
3-azaspiro [5, 5] undecan-3-aminium chloride	56.0±10.5	14.7±3.2
ASDI TO500-7514	36.2±4.5	25.5±5.9
1-Ad-CH2-OH	61.8±6.3	40.9±7.1

Amounts of remaining activity of A/M2 channel after the inhibition with various compounds at 100 μM. Responses in the presence of a drug were normalized to the currents measured in absence of a drug. Each value is a mean (±SD) of 2–3 independent experiments

copper interactions with ligating sidechains such as Cys and His in various proteins including ion channels and transporters potentially conducting protons in A/M2-free CHO-K1 membranes [37]. Besides, the pH-induced amantadine-insensitive currents may also result from charging of the sensor surface due to transporter-independent protonation of adsorbed membrane proteins. This assumption is supported by the observation that no significant pH-induced currents were detected with sensors prepared with empty liposomes, whereas the channel activity of A/M2 proteins reconstituted in liposomes was similar to that measured for A/M2 expressing CHO-K1 cells (Electronic supplementary material). In order to better differentiate between the A/M2-specific response and the pH-induced endogenous activity of CHO-K1 cell membranes, the Cu(II)-insensitive component of the current was subtracted from the total pH-induced current. By doing so, the total fraction of the current inhibited by 100 μM amantadine became comparable to the values detected with either TEVC on A/M2 channels expressed in *Xenopus* oocytes (Fig. 1b), or with the whole-cell configuration of the patch-clamp technique on A/M2 channels expressed in CHO-K1 cells [25]. Based on these findings, we conclude that SSM-based assay is capable of measuring the A/M2-specific signal and to distinguish it from the background activity of the A/M2 expressing system.

A/M2 channel ion selectivity A/M2 channels show high selectivity for protons over other monovalent cations [15, 27]. In TEVC experiments on A/M2 channels expressed in *Xenopus* oocytes, the reversal voltage and the amount of current did not change significantly when measured in either Na^+-, K^+-, or $NMDG^+$-based solutions (Fig. 2a). Consistent with the electrophysiological results, A/M2 channels assayed using SSM-based technology did not show any conductance differences when activated in the presence of either K^+, or impermeable $NMDG^+$ (Fig. 2b). By these experiments, we confirmed that with the SSM-based assay A/M2 specific proton current is detected.

A/M2 channel amantadine sensitivity Amantadine is a hydrophobic drug, with a molecular cross-section of 4—5 Å—significantly larger than the small (approximately 2–3 Å) opening at the entry of the pore observed in the NMR and crystal structures of the protein [38, 39]. This finding suggests that the drug must enter and exit the channel via rare conformational transitions. This conclusion is consistent with the observation that association of the drug occurs with a second-order rate constant that is at least 10^4-fold slower than the diffusion-controlled rate. Moreover, the channel undergoes rapid conformational fluctuations in the micro to millisecond time scale in both the drug free and amantadine-bound states [40–42] and the dynamics [11] and malleability [32] of the channel are also well known to be strongly influenced changes in the lipid environment. Thus, it is hardly surprising that there is a twofold difference between the first-order rate constant for loss of inhibition (k_{off}) observed between electrophysiologically assayed A/M2 expressing oocytes and CHO-K1 cells, or a much higher difference in k_{off} between the patch-clamped whole CHO-K1 cells and isolated membranes immobilized on the SSM-coated sensors. Indeed, the difference for whole CHO-K1 cells vs. isolated membranes represents a difference in activation energy of only two times thermal energy at room temperature.

The more rapid equilibration time for isolated membranes has serendipitous effects for screening of drug interactions, enabling measurements of IC_{50} values that more accurately reflect the true affinity of inhibitors for A/M2. Previous electrophysiological measurements of inhibition have been temporally limited by the finite lifetime of both M2-expressing cells as well as the seal to the cell, practically limiting compound incubation times to a few minutes for routine measurements. The relaxation rate for inhibition of a channel is given by $k_{inh} = k_{on}[drug] + k_{off}$. In oocytes, k_{on} is approximately 10^3 M^{-1} s^{-1} for amantadine binding to A/M2 protein from the A/Udorn/72 influenza A virus strain studied here and k_{off} is approximately 10^{-4} s^{-1} [28]. Thus, the half-time for reaching equilibrium at 100 μM drug concentration is approximately 0.1 min, but increases to 10 min at 1 μM and 1 h at 0.1 μM. Thus, it is not routinely possible to reach equilibrium at low drug concentrations, and the IC_{50} values measured after 2-min incubation time are artificially increased. The more rapid apparent equilibration time observed in the SSM-based method explains the lower IC_{50} of 0.3 μM observed for amantadine relative to the value of 5 to 16 μM obtained by the conventional electrophysiological measurements with mammalian cells and oocytes. Although an extensive set of data are not available, it would appear that the value of 0.3 μM is close to the true IC_{50}, because, in one published experiment that examines extended incubation times in oocytes, 0.4 μM amantadine is sufficient to give approximately 50% inhibition of A/M2 after a 1-h period. Thus, the more rapid off-rate observed for the SSM is likely to reflect primarily a difference in kinetics rather than equilibrium.

Inhibition pattern of amantadine-insensitive mutants While efficiently inhibiting wild-type A/M2 channel activity, physiologically relevant amantadine concentrations do not alter the activity of the A/M2-S31N and A/M2-V27A mutant channels. These mutations occur naturally in circulating A/M2 virus strains, causing amantadine to become ineffective in preventing viral replication [8–10, 12, 13]. Here, we confirmed that A/M2-S31N and A/M2-

V27A mutants do not show amantadine sensitivity when assayed with the SSM-based technology (Fig. 5).

Spiro[5.5]undecan-3-amine (spiran amine) was recently shown to inhibit selectively the activity of A/M2-V27A amantadine-insensitive mutant, while remaining ineffective for the inhibition of A/M2-S31N channels [34]. The inhibition potency of the spiran amine compound on A/M2 wild-type and mutant channels was also assayed with the SSM-based technique (Fig. 5a). The inhibition by the drugs of the tested channels was not significantly different between the SSM-based assay and the TEVC measurements (Fig. 5b). The consistency between the two assays indicates that the SSM-technology can be reliably used for the investigation of A/M2 wild-type and mutant channel inhibitors, although larger scale study is needed.

Inhibition potencies of anti-viral compounds on A/M2 The reliability of the SSM-based technology for the larger scale screening assays was confirmed by testing nine additional chemical compounds, which were previously shown to be effective, or ineffective for the inhibition of A/M2 channel activity [16, 34–36]. The inhibition results obtained with SSM-based technology were not significantly different from those obtained using TEVC (Table 1). The consistency of the inhibition trends between the two techniques indicates that the tested compounds did not interfere with the SSM assay. Thus, these results show that the SSM-based technology may safely be applied in screening for potential A/M2 channel modulators.

Conclusions

In this work, we validated the use of the SSM-based technology for the investigation of ion channel activity and its potential for use in screening for new drugs. The study shows that the SSM-based assay gives reliable and reproducible results that correctly reflect A/M2 channel behavior measured conventionally. Moreover, the SSM-based A/M2 assay is more sensitive when compared with the usually applied conventional TEVC using oocytes.

We believe that SSM-based electrophysiology will become a valuable tool in the ion channel research toolbox.

Materials and methods

Molecular biology, in vitro cRNA transcription and transient expression in CHO-K1 cultured cells The cDNA encoding to the Influenza virus A/Udorn/72 A/M2 protein and to the A/M2-S31N, A/M2H37G, A/M2-V27A mutants were inserted into pGEMHJ (a gift from N. Dascal Tel-Aviv University, Israel) for the expression on *Xenopus* oocytes or to the pCAGGS [43] for the expression in CHO-K1 cells. For the generation of A/M2-pHluorin construct, the DNA fragment-encoding pHluorin was prepared from pHluorin-pGEX-2T plasmid (a gift from G. Miesenböck, Yele University, CT) by standard PCR, the amplified fragments were linked to the C-terminus of A/M2 as previously described [44] (see Electronic supplementary material). The regions amplified by PCR were verified by double-strand DNA sequencing. In all cases numbering of amino acids starts from the first methionine of ORF. cRNA was prepared as previously described [44]. CHO-K1 cells (Clontech, Mountain View, CA) were cultured as previously described [25]. Transfections were done on 30%–50% confluent cultures using *Lipofectamine 2000* reagent (Invitrogen, Grand Island, NY) with 5 μg/dish total plasmid cDNA.

Heterologous expression and TEVC measurements from xenopus oocytes Stage V–VI *Xenopus laevis* oocytes were prepared as described previously [15]. Oocytes were injected with 5–10 ng of cRNA in 50 nl/oocyte, and assayed 2–3 days later. Two electrode voltage clamp recordings were carried out using TEV-200 (Dagan, Minneapolis, MN) connected to DIGIDATA 1440A and pCLAMP10 (Molecular Devises, Sunnyvale, CA). Oocytes were superfused with Ca^{2+}-free normal frog Ringer's solution (in millimolars) 115 NaCl, 2.5 KCl, 1.8 MgCl2, and 15 HEPES for pH 8.5 or 15 MES for pH 5.5. For the ion selectivity measurements, Na^+ in the recording solution was replaced by either K^+ or $NMDG^+$. Currents were recorded at −20 mV. Amantadine (100 μM; Sigma, St. Louis, MO) was applied to inhibit A/M2-induced currents. Data were analyzed using ORIGIN 8.0 software (OriginLab, Northampton, MA). Other A/M2 channel inhibitors were synthesized in-house [16, 34].

Whole-cell patch-clamp measurements Macroscopic currents were recorded in the whole-cell configuration at room temperature (22–24°C) and at the holding potential of 0 mV as previously described [25]. The non-activating solution contained (in millimolars): NMDG (135), HEPES (25), $CaCl_2$ (5), glucose (10; pH 7.4). The activating solution contained in millimolars: NMDG (135), MES (25), $CaCl_2$ (5), glucose (10; pH 6.0). For inhibiting A/M2 channel activity, the appropriate concentration of amantadine was added to the non-activating solution. The recorded data was analyzed and plotted using Matlab 2008.

Fluorescence intensity measurements pHluorin emission was recorded simultaneously with whole-cell membrane currents to estimate the intracellular pH [33]. Briefly, pHluorin was excited with 410 and 470 nm wavelengths and ratio of the emission intensities R410/470 was recorded. Fluorescence was measured using a PTI Image

Master microfluorometer system (Photon Technology International, NJ, USA) with a ×40 0.6 NA objective on an Olympus IMT-2 microscope. The sampling time was about 11 s. Intensity quantifications were done using the software Image Master 5.0 in arbitrary units.

Preparation of CHO membranes The A/M2 proteins were transiently expressed in CHO-K1 cells and the corresponding CHO-K1 membranes were prepared by sucrose step centrifugation as follows. CHO cell pellet (~0.15 g wet weight) was rapidly melted and resuspended in ice-cold 500 μL of sucrose buffer (250 mM sucrose, 10 mM Tris, pH 7.5, protease inhibitor mix "*Complete EDTA free*" (Roche)). The cells were broken on ice using a glass dounce-homogenizer and the resulting suspension was centrifuged for 10 min at 5,000×*g* and 4°C. The supernatant was collected and centrifuged for 30 min at 100.000×*g* and 4°C. The resulting pellet was resuspended in 50 μL of ice-cold 10 mM Tris (pH 7.5) and sucrose to a final concentration of 51% (*w*/*v*). Then, the same volume of 45% and of 9% sucrose (*w*/*v* in 10 mM Tris, pH 7.5) were stacked layer by layer on the 51% suspension, and the gradient was centrifuged for 2.5 h at 100.000×*g* and 4°C in SW41 rotor (Beckman Coulter, USA). The membranes in 9/45% interphase were collected, mixed with 5 volumes of ice-cold storing buffer (30 mM NaCl, 0.5 mM EDTA, 10 mM Tris, pH 7.5), and centrifuged for 30 min at 100.000×*g* and 4°C. The final pellet was resuspended in 20 μL of storing buffer containing 5% glycerol and 0.2 mM DTT. The total protein concentration of the obtained membrane suspension was usually in the range of 5–10 μg protein/μl. The membranes were aliquotted, frozen in liquid nitrogen, and stored at −80°C.

SSM-based biosensors and measurements The biosensors were prepared with single-gold-electrode sensors from IonGate Biosciences (Germany) as described by the manufacturer. Briefly, the SSM was built on the gold electrode by applying first an alkane-thiol monolayer followed by a phospholipid (di-phytanoyl-phosphatidyl-choline) monolayer on top of it. Accordingly, the lipid and the alkane-thiol form a composite bilayer with the phospholipid monolayer facing the aqueous solution. Subsequently, these SSM-coated sensors were covered with 50 μL of the ice-cold M2 sensor preparation buffer (30 mM MES/KOH, pH 5.8, 140 KCl, 4 mM MgCl2, 0.2 mM DTT) and incubated at 4°C for 15 min. An aliquot of CHO-K1 membranes was rapidly melted, diluted with the sensor preparation buffer to a final protein concentration of 0.5–1 μg/μL, and sonicated with a microsonicator by applying five bursts with an amplitude of 30% (ultrasonic processor UP 50 H with a MS 1 tip, Dr. Hielscher, Germany). Five to ten micrograms of total protein of the sonicated membranes were loaded per each sensor, centrifuged for 30 min at 2,000×*g* and 4°C, and incubated for 2–48 h at 4°C.

After this incubation the sensors could be stored for another 48 h at 4°C without significant reduction of the protein activities. For electrical measurements, the membrane-loaded biosensors were integrated into the fluidic system of the *SURFE*^{2}*R* device (Surface Electrogenic Event Reader, IonGate Biosciences, Germany), and the A/M2 was activated through pH jumps by exchanging the "non-activating" solution (30 mM MOPS/KOH, pH 7.0, 140 KCl, 4 mM MgCl2) for the "activating" solution (30 mM MES/KOH, pH 6.0, 140 KCl, 4 mM MgCl2). The system was set back to the original inactivated state by rinsing the sensor with the non-activating solution. After equilibrating the sensor for ≥30 s in the non-activating solution, the A/M2 protein could be activated again by applying the activating solution. Like this, the A/M2 protein could be repeatedly activated over an extended time period. The possible changes (drift) of the protein activity during the experimental period were monitored by application of a reference activating solution.

For the inhibition experiments, all test inhibitors were supplied at the same concentration to both activating and non-activating solutions. After recording the current in the absence of inhibitor the currents were first inhibited with the test inhibitor, then, after washout with the non-activating solution, sensors were exposed to amantadine (100 μM) to control the inhibition level, washed out, and exposed to Cu(II) (25 μM). The order in which solutions were presented to the SSM sensor follows: (1) non-activating solution, (2) activating solution, (3) non-activating solution with test inhibitor, (4) activating solution with test inhibitor, (5) washout with non-activating solution, (6) non-activating solution with amantadine, (7) activating solution with amantadine, (8) washout with non-activating solution, (9) non-activating solution with Cu(II), and (10) activating solution with Cu(II). The inhibitory effect of Cu(II) is not reversible in the time course of these experiments, and a new sensor needs to be used for the next measurements.

Acknowledgements The research was supported by the National Institute of Health research grants R01 AI-57363 (L.H.P.), R01 AI-74517 (W.F.D. and J.W), U01 AI1074571 (L.H.P. and W.F.D.) and by the National Science Foundation research grant DBI-0551852 (S.I.) and GM56416 (W.F.D. and J.W).

References

1. Cox NJ, Subbarao K (1999) Influenza. Lancet 354:1277–1282
2. Lamb RA, Zebedee SL, Richardson CD (1985) Influenza virus M2 protein is an integral membrane protein expressed on the infected-cell surface. Cell 40:627–633

3. Lamb RA, Holsinger LJ, Pinto LH (1994) The influenza A virus M2 ion channel protein and its role in the influenza virus life cycle. In: Wimmer E (ed) Receptor-mediated virus entry into cells. Cold Spring Harbor Laboratory Press, Cold Spring Harbor, pp 303–321
4. Tang Y, Venkataraman P, Knopman J, Lamb RA, Pinto LH (2005) The M2 proteins of Influenza A and B viruses are single-pass proton channels. In: Fischer WB (ed) Viral membrane proteins: structure, function and drug design. Kluwer Academic/Plenum Publisher, New York, pp 101–111
5. Pinto LH, Lamb RA (2007) Controlling influenza virus replication by inhibiting its proton channel. Mol Biosyst 3:18–23
6. Pinto LH, Lamb RA (2006) The M2 proton channels of influenza A and B viruses. J Biol Chem 281:8997–9000
7. Hu J, Fu R, Nishimura K, Zhang L, Zhou HX, Busath DD, Vijayvergiya V, Cross TA (2006) Histidines, heart of the hydrogen ion channel from influenza A virus: toward an understanding of conductance and proton selectivity. Proc Natl Acad Sci USA 103:6865–6870
8. Bright RA, Shay DK, Shu B, Cox NJ, Klimov AI (2006) Adamantane resistance among influenza A viruses isolated early during the 2005–2006 influenza season in the United States. JAMA 295:891–894
9. Deyde VM, Xu X, Bright RA, Shaw M, Smith CB, Zhang Y, Shu Y, Gubareva LV, Cox NJ, Klimov AI (2007) Surveillance of resistance to adamantanes among influenza A(H3N2) and A (H1N1) viruses isolated worldwide. J Infect Dis 196:249–257
10. Hay AJ, Wolstenholme AJ, Skehel JJ, Smith MH (1985) The molecular basis of the specific anti-influenza action of amantadine. EMBO J 4:3021–3024
11. Cady SD, Mishanina TV, Hong M (2009) Structure of amantadine-bound M2 transmembrane peptide of influenza A in lipid bilayers from magic-angle-spinning solid-state NMR: the role of Ser31 in amantadine binding. J Mol Biol 385:1127–1141
12. Bright RA, Medina MJ, Xu X, Perez-Oronoz G, Wallis TR, Davis XM, Povinelli L, Cox NJ, Klimov AI (2005) Incidence of adamantane resistance among influenza A (H3N2) viruses isolated worldwide from 1994 to 2005: a cause for concern. Lancet 366:1175–1181
13. Saito R, Sakai T, Sato I, Sano Y, Oshitani H, Sato M, Suzuki H (2003) Frequency of amantadine-resistant influenza A viruses during two seasons featuring cocirculation of H1N1 and H3N2. J Clin Microbiol 41:2164–2165
14. Mould JA, Paterson RG, Takeda M, Ohigashi Y, Venkataraman P, Lamb RA, Pinto LH (2003) Influenza B virus BM2 protein has ion channel activity that conducts protons across membranes. Dev Cell 5:175–184
15. Shimbo K, Brassard DL, Lamb RA, Pinto LH (1996) Ion selectivity and activation of the M2 ion channel of influenza virus. Biophys J 70:1335–1346
16. Wang J, Cady SD, Balannik V, Pinto LH, DeGrado WF, Hong M (2009) Discovery of spiro-piperidine inhibitors and their modulation of the dynamics of the M2 proton channel from influenza A virus. J Am Chem Soc 131:8066–8076
17. Pintschovius J, Fendler K (1999) Charge translocation by the Na+/K+-ATPase investigated on solid supported membranes: rapid solution exchange with a new technique. Biophys J 76:814–826
18. Schulz P, Garcia-Celma JJ, Fendler K (2008) SSM-based electrophysiology. Methods 46:97–103
19. Ganea C, Fendler K (2009) Bacterial transporters: charge translocation and mechanism. Biochim Biophys Acta 1787 (6):706–13
20. Garcia-Celma JJ, Smirnova IN, Kaback HR, Fendler K (2009) Electrophysiological characterization of LacY. Proc Natl Acad Sci USA 106:7373–7378
21. Kelety B, Diekert K, Tobien J, Watzke N, Dorner W, Obrdlik P, Fendler K (2006) Transporter assays using solid supported membranes: a novel screening platform for drug discovery. Assay Drug Dev Technol 4:575–582
22. Krause R, Watzke N, Kelety B, Dorner W, Fendler K (2009) An automatic electrophysiological assay for the neuronal glutamate transporter mEAAC1. J Neurosci Methods 177:131–141
23. Weitz D, Harder D, Casagrande F, Fotiadis D, Obrdlik P, Kelety B, Daniel H (2007) Functional and structural characterization of a prokaryotic peptide transporter with features similar to mammalian PEPT1. J Biol Chem 282:2832–2839
24. Schulz P, Dueck B, Mourot A, Hatahet L, Fendler K (2009) Measuring ion channels on solid supported membranes. Biophys J 97:388–396
25. Jing X, Ma C, Ohigashi Y, Oliveira FA, Jardetzky TS, Pinto LH, Lamb RA (2008) Functional studies indicate amantadine binds to the pore of the influenza A virus M2 proton-selective ion channel. Proc Natl Acad Sci USA 105:10967–10972
26. Gandhi CS, Shuck K, Lear JD, Dieckmann GR, DeGrado WF, Lamb RA, Pinto LH (1999) Cu(II) inhibition of the proton translocation machinery of the influenza A virus M2 protein. J Biol Chem 274:5474–5482
27. Chizhmakov IV, Geraghty FM, Ogden DC, Hayhurst A, Antoniou M, Hay AJ (1996) Selective proton permeability and pH regulation of the influenza virus M2 channel expressed in mouse erythroleukaemia cells. J Physiol 494(Pt 2):329–336
28. Wang C, Takeuchi K, Pinto LH, Lamb RA (1993) Ion channel activity of influenza A virus M2 protein: characterization of the amantadine block. J Virol 67:5585–5594
29. Lin TI, Schroeder C (2001) Definitive assignment of proton selectivity and attoampere unitary current to the M2 ion channel protein of influenza A virus. J Virol 75:3647–3656
30. Schroeder C, Ford CM, Wharton SA, Hay AJ (1994) Functional reconstitution in lipid vesicles of influenza virus M2 protein expressed by baculovirus: evidence for proton transfer activity. J Gen Virol 75(Pt 12):3477–3484
31. Skehel JJ, Hay AJ, Armstrong JA (1978) On the mechanism of inhibition of influenza virus replication by amantadine hydrochloride. J Gen Virol 38:97–110
32. Stouffer AL, Ma C, Cristian L, Ohigashi Y, Lamb RA, Lear JD, Pinto LH, DeGrado WF (2008) The interplay of functional tuning, drug resistance, and thermodynamic stability in the evolution of the M2 proton channel from the influenza A virus. Structure 16:1067–1076
33. Miesenbock G, De Angelis DA, Rothman JE (1998) Visualizing secretion and synaptic transmission with pH-sensitive green fluorescent proteins. Nature 394:192–195
34. Balannik V, Wang J, Jing X, Magavern E, Lamb RA, DeGrado WF, Pinto LH (2009) Design and pharmacological characterization of inhibitors of amantadine-resistant mutants of the m2 ion channel of influenza A virus. Biochemistry (in press)
35. Tu Q, Pinto LH, Luo G, Shaughnessy MA, Mullaney D, Kurtz S, Krystal M, Lamb RA (1996) Characterization of inhibition of M2 ion channel activity by BL-1743, an inhibitor of influenza A virus. J Virol 70:4246–4252
36. Kolocouris A, Spearpoint P, Martin SR, Hay AJ, Lopez-Querol M, Sureda FX, Padalko E, Neyts J, De Clercq E (2008) Comparisons of the influenza virus A M2 channel binding affinities, anti-influenza virus potencies and NMDA antagonistic activities of 2-alkyl-2-aminoadamantanes and analogues. Bioorg Med Chem Lett 18:6156–6160
37. Goldstein S, Czapski G (1986) The role and mechanism of metal ions and their complexes in enhancing damage in biological

systems or in protecting these systems from the toxicity of O2. J Free Radic Biol Med 2:3–11
38. Schnell JR, Chou JJ (2008) Structure and mechanism of the M2 proton channel of influenza A virus. Nature 451:591–595
39. Stouffer AL, Acharya R, Salom D, Levine AS, Di Costanzo L, Soto CS, Tereshko V, Nanda V, Stayrook S, DeGrado WF (2008) Structural basis for the function and inhibition of an influenza virus proton channel. Nature 451:596–599
40. Li C, Qin H, Gao FP, Cross TA (2007) Solid-state NMR characterization of conformational plasticity within the transmembrane domain of the influenza A M2 proton channel. Biochim Biophys Acta 1768:3162–3170
41. Yi M, Cross TA, Zhou HX (2008) A secondary gate as a mechanism for inhibition of the M2 proton channel by amantadine. J Phys Chem B 112:7977–7979
42. Yi M, Cross TA, Zhou HX (2009) Conformational heterogeneity of the M2 proton channel and a structural model for channel activation. Proc Natl Acad Sci USA 106:13311–13316
43. Niwa H, Yamamura K, Miyazaki J (1991) Efficient selection for high-expression transfectants with a novel eukaryotic vector. Gene 108:193–199
44. Balannik V, Lamb RA, Pinto LH (2008) The oligomeric state of the active BM2 ion channel protein of influenza B virus. J Biol Chem 283:4895–4904